Biodegradation (2007) 18:693–701
DOI 10.1007/s10532-007-9106-x

ORIGINAL PAPER

Modeling bio-protection and the gradient-resistance mechanism

Alex O. Schwarz · Bruce E. Rittmann

Received: 23 August 2006 / Accepted: 24 January 2007 / Published online: 21 February 2007

Abstract We expand the biogeochemical program CCBATCH to describe transport processes in 1-D ground-water systems. We use the expanded CCBATCH with our biogeochemical framework for metal detoxification in sulfidic systems to study complex bio-protection scenarios. In particular, in our numerical experiments we expose a consortium of sulfate-reducing bacteria and fermenting bacteria to a toxic concentration of Zn^{2+} in a 1-D system with precipitation of zinc-sulfide solids turned off or on. Our results confirm the key role of sulfide precipitation in detoxification when coupled effects of transport and biological processes are considered. The potential of sulfide as a detoxifying agent in bio-protection is explained by its high mobility, its high affinity for metals, and its high rate of production in sulfidic systems. Thus, our numerical results offer important evidence for the gradient-resistance mechanism and validate that a metal-resistance criterion developed from an analytical solution is accurate for defining when bio-protection should succeed.

Keywords Biogeochemical model · Bio-protection · Metal speciation · Metal detoxification · Sulfidic systems · Toxic metals

A. O. Schwarz (✉)
Department of Civil Engineering, University of Concepción, Casilla 160-C, Correo 3, Ciudad Universitaria, Concepción, Chile
e-mail: alexschwarz@udec.cl

B. E. Rittmann
Center for Environmental Biotechnology, Biodesign Institute at Arizona State University, 1001 South McAllister Ave., Tempe, AZ 85287-5701, USA
e-mail: Rittmann@asu.edu

A. O. Schwarz · B. E. Rittmann
Department of Civil and Environmental Engineering, Northwestern University, 2145 Sheridan Road, Evanston, IL 60208-3109, USA

A. O. Schwarz
e-mail: alexschwarz@udec.cl

B. E. Rittmann
e-mail: Rittmann@asu.edu

Introduction

A general metals bio-protection mechanism, of widespread applicability to microbial communities, occurs when some bacteria in the community induce pore-water metal gradients by producing ligands that bind the metal toxicant, reducing its concentration to non-inhibitory levels for much of the community. Our prior work has laid the foundation for understanding this bio-protection mechanism in a quantitative way. In particular, we developed a biogeochemical framework that comprehensively describes the reactivity of biological and geochemical components in sulfidic

systems and implemented this framework in the biogeochemical model CCBATCH (Schwarz and Rittmann 2007). Using analytical modeling, we also developed relationships that predict when toxicity resistance due to chemical gradients ought to be possible (Schwarz and Rittmann 2006).

The numerical experiments we present in this contribution capitalize on our other findings. Here, we expand CCBATCH to model the transport processes involved in the movement of metals and ligands in aqueous systems. It is essential that we add transport, because transport resistance is responsible for the formation of chemical gradients in the bio-protection mechanism (Schwarz and Rittmann 2006). Specifically, we use the biogeochemical framework, including transport processes, for understanding and quantitatively evaluating metals bio-protection in a sulfidic permeable reactive barrier (PRB). The numerical approach lets us evaluate more realistic settings than we could using analytical tools. The analytical results, however, are particularly useful here, because they provide simple relationships that can be tested under the more realistic conditions and also are useful to parameterize the numerical model.

Within the complex microbial communities of sulfidic systems, sulfate-reducing bacteria (SRB) are outstanding candidates for inducing the necessary pore-water metal gradients to bio-protect the entire community, because they produce sulfide, which forms strong complexes and sparingly soluble precipitates with many toxic metals. Thus, our goal is to clarify the role of sulfide in detoxification when the coupled effects of transport and biological processes are considered, particularly when we simulate the exposure of a consortium of SRB and fermenting bacteria to toxic concentrations of Zn in a one-dimensional (1-D) ground-water environment.

Description of the modeled system

Our 1-D numerical experiments are designed to differentiate among different detoxification reactions and address biological complexity in bio-protection applications. The conceptual model we designed for our simulations is shown in Fig. 1. The selected domain can represent, for example, the up-gradient boundary of a full-scale PRB designed for toxic-metal containment. The toxic metal enters the biologically active zone (BAZ) from the left by advection. The detoxifying ligand is produced in the BAZ to the right and diffuses to the left. The ligand and metal react to form non-toxic species (e.g., solids or complexes) where the two reactants meet, and this reaction consumes the metal and the ligand, setting up the gradients of both. The gradient for the toxic metal lowers its concentration so that biological activity can be sustained within the BAZ.

We assume an average ground-water velocity of 5 m y^{-1} and model a 15-cm PRB segment with a segment of up-gradient neighboring aquifer of the same length and hydraulic characteristics. It is unnecessary to model the entire PRB, since, for bio-protection applications and as shown in the analytical solution examples (Schwarz and Rittmann 2006), what matters is the accurate representation of the failure mechanism, which is initiated at the up-gradient boundary. If the metal concentration within the up-gradient region of the BAZ increases to toxic levels, less ligand is produced to immobilize/detoxify the metal, and the metal concentration continues to increase, ultimately leading to down-gradient movement of the metal, complete inhibition of the BAZ, and failure of bio-protection by gradient resistance.

Our previous analytical analysis (Schwarz and Rittmann 2006) showed that the bio-protection mechanism can only work for relatively low ground-water velocities. Hence, although ground-water velocities can be several orders of magnitude higher, we selected a relatively low value of 5 m y^{-1} to allow bio-protection for typical sulfidogenic PRB conditions (Benner

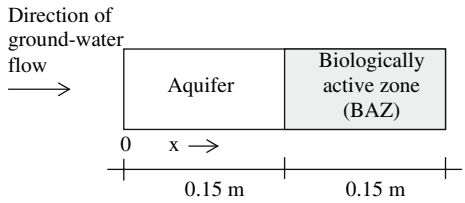

Fig. 1 Physical set-up for the 1-D numerical experiments. A biologically active zone (BAZ) of sulfide generation is exposed to Zn toxicity

et al. 2002). On the other hand, homogeneity over 15 cm is relevant for the field, because PRBs are relatively homogeneous and typically preceded by segments of granular material to homogenize the flow approaching the PRB.

The influent ground water resembles typical freshwater (Stumm and Morgan 1996) (Table 1). The key metal-detoxification mechanisms modeled are complexation to microbial products, complexation to sulfide, and precipitation with sulfide. We assume that free Zn (Zn^{2+}) is the toxic Zn species (Campbell 1995; Campbell et al. 2002; Paquin et al. 2002). Compared to advection, all detoxification reactions are assumed to be fast, and, therefore, they are modeled as equilibrium reactions. Finally, mixing is modeled using an effective diffusion coefficient, because back-transport due to diffusion is fundamental to resistance based on a chemical gradient. Mixing due to dispersion is less relevant for this analysis and is not considered.

Sulfidogenic PRBs typically use a mixture of celullosic and lignocellulosic materials (e.g., leaf mulch, wood chips, or sawdust) as electron-donor sources (Waybrant et al. 2002). Importantly, hydrolysis rates of these materials are low enough so that hydrolysis controls overall degradation kinetics (Rittmann and McCarty 2001), as long as the electron acceptor, sulfate in our case, is not limiting. Because hydrolysis controls the degradation kinetics, we do not need to consider intermediates (e.g., hydrogen and acetate). Thus, lignocellulosic particles are the rate-limiting donor material, which allows important simplifications of the biological model.

Table 1 Parameter values used in 1-D simulations

Parameter	Symbol	Unit	Value
Influent total Zn concentration	$[Zn]_T$	M	50×10^{-6}
Influent pH	pH_0	–	7.1
Influent total carbonate concentration	$[CO_3^{2-}]_T$	M	2×10^{-3}
Influent total chloride concentration	$[Cl^-]_T$	M	2.5×10^{-4}
Influent total calcium concentration	$[Ca^{2+}]_T$	M	1×10^{-3}
Influent total magnesium concentration	$[Mg^{2+}]_T$	M	3×10^{-4}
Influent total sodium concentration	$[Na^+]_T$	M	2.5×10^{-4}
Influent total ammonium concentration	$[NH_4^+]_T$	M	1×10^{-3}
Influent total sulfate concentration	$[SO_4^{2-}]_T$	M	1×10^{-3}
Effective diffusion coefficient	D	$m^2\ d^{-1}$	1×10^{-4}
Hydrolysis rate of lignocellulosic material	k_{hl}	mol $l^{-1}\ d^{-1}$	4.75×10^{-5}
Domain length	L_d	m	0.3

Table 2 presents the stoichiometry for the biological model we use in this numerical experiment, for which only hydrolysis limits biodegradation. All the biochemical reactions included in Table 1 in Schwarz and Rittmann (2007) are represented in Table 2 here; however, simplification comes about as reactions in Table 1 in Schwarz and Rittmann (2007) are multiplied by appropriate stoichiometric factors and summed up to obtain the reactions in Table 2 here. For example, the three steps for the complete mineralization of cellulose are: cellulose conversion to H_2 and acetate, H_2 oxidation, and acetate mineralization. We obtain the stoichiometric coefficients for the overall reaction (Reaction 1 in Table 2 here) by summing the stoichiometric coefficients for each species appearing in all intermediate steps. The key is to cancel out overall stoichiometric factors of H_2 and acetate, because they are consumed as fast as they are produced. To cancel out the overall stoichiometric factor of H_2, we multiply the stoichiometric factors of the H_2 mineralization step by the negative of the H_2 stoichiometric factor from the cellulose fermentation step. Additionally, to cancel out the overall stoichiometric factor of acetate, we multiply the stoichiometric factors of the acetate mineralization reaction by the negative of the sum of acetate stoichiometric factors from the first two reactions. In this way, H_2 and acetate disappear when all steps are summed. A second simplification comes about as biomass respiration and inactivation reactions are summed up to give an overall biomass endogenous decay reaction for each active biomass type (Reactions 2, 3 and 4). An overall endogenous decay reaction is only possible when biomass respiration is not electron-acceptor (i.e., sulfate) limited, as is assumed in our analysis, and biomass respiration and inactivation reactions share the same kinetics.

Table 2 Matrix of stoichiometry for the simplified representation of a sulfidic system

Reaction	Cellulose	SO_4^{2-}	H_2S	H^+	H_2CO_3	NH_4^+	X_F	X_H	X_A	X_I	EPS	UAP	BAP
1. Cellulose degradation	–1	–2.1055	2.1055	–3.8528	4.2108	–0.3579	0.1117	0.0522	0.0258	0	0.1324	0.0358	0
2. Fermenter endogenous decay	0	–1.7027	1.7027	–4.0863	3.4052	0.681	–1	0.0423	0.0208	0.2	0.044	0.0119	0
3. H_2–SRB endogenous decay	0	–2	2	–4.8	4	0.8	0	–1	0	0.2	0	0	0
4. Acetate-SRB endogenous decay	0	–2	2	–4.8	4	0.8	0	0	–1	0.2	0	0	0
5. UAP degradation	0	–1.7027	1.7027	–4.0863	3.4052	0.681	0.1178	0.047	0.0231	0	0.1311	–1	0
6. BAP degradation	0	–1.7027	1.7027	–4.0863	3.4052	0.681	0.1178	0.047	0.0231	0	0.1311	0	–1
7. BAP formation	0	0	0	0	0	0	0	0	0	0	–1	0	1

Definitions: X_F is active biomass of fermenting bacteria, X_A is active biomass of acetate-utilizing SRB (acetate-SRB), X_H is active biomass of hydrogen-utilizing SRB (H_2-SRB), X_I is true residual inert biomass, EPS is extracellular polymeric substances, UAP is utilization associated products, and BAP is biomass associated products

Assumptions: ammonium is the nitrogen source in all synthesis reactions; in cellulose fermentation, 67% of the electrons shuttled to products end up in acetate, with the other 33% in H_2; in H_2 oxidation, 67% of the carbon for synthesis comes from acetate and 33% from H_2CO_3; 53% of substrate electrons are diverted toward active biomass, 37% toward EPS, and 10% toward UAP; the biodegradable fraction of the active biomass f_d is 80%; and, H_2-SRB endogenous respiration and acetate-SRB endogenous respiration are not sulfate-limited. We take into account reaction energetics to determine the true yield coefficients Y_F, Y_H and Y_A, which are key parameters of the matrix of stoichiometry listed in Table 1 of Schwarz and Rittmann (2007). The procedure of balancing microbial reactions is detailed in Rittmann and McCarty (2001)

We determine the value for the hydrolysis rate constant k_{hl} in Table 1 by beginning with an observed sulfate-reduction rate of 10^{-4} mol l^{-1} d^{-1} and then dividing by the stoichiometric factor for sulfate reduction linked to donor utilization (2.1055 mol SO_4^{2-}/mol-cellulose in the first reaction of Table 2). The selected sulfate-reduction rate is at the low end of the range of 1.1×10^{-4} to 1.6×10^{-4} mol l^{-1} d^{-1} reported by Benner et al. (2002) for a sulfidic PRB.

As explained in Schwarz and Rittmann (2007), microbial products display significant and varied reactivity toward metals, and, thus, they need to be accounted for by biogeochemical models. In our analysis, steady-state biomass concentrations of consortium members result from the balance of substrate-utilization and endogenous decay. A first approximation for the steady-state active biomass can be obtained from the following differential mass balance equation:

$$\frac{dX_{ai}}{dt} = 0 = \lambda_i k_{hl} - b_i X_{ai} \quad \text{giving } X_{ai} = \frac{\lambda_i k_{hl}}{b_i} \qquad (1)$$

where X_{ai} is the steady-state active biomass of type i (M_x), k_{hl} is the hydrolysis rate of lignocellulosic material ($M_g L^{-3} T^{-1}$), λ_i is the stoichiometric coefficient for biomass type i ($M_x M_g^{-1}$) (from the first reaction in Table 2), and b_i is the endogenous decay coefficient for biomass type i (T^{-1}). The values of b_i depend on species type and temperature, but they are not generally reported in the literature. Hence, we assume the same b_i value of 0.05 d^{-1}, typical of slow-growing species (Rittmann and McCarty 2001), for all populations, when we compute the concentrations of steady-state biomass that are synthesized from substrate utilization: $X_F = 1.06 \times 10^{-4}$ M, $X_A = 2.45 \times 10^{-5}$ M, and $X_H = 4.96 \times 10^{-5}$ M. X_F is by far the most abundant type of biomass, with X_A the least abundant. Inert biomass does not reach a steady-state concentration, because it continually increases. The steady-state concentration of EPS can be obtained using an expression similar to Eq. 1 with the first-order hydrolysis rate coefficient of EPS ($k_{hyd} = 0.17$ d^{-1}) (Schwarz and Rittmann 2007) in the denominator instead of the endogenous decay coefficient; this gives $EPS = 3.7 \times 10^{-5}$ M.

Solution approach including transport

For the PRB examples, we expand CCBATCH to include transport. We solve the following equations governing transport and reactivity, based on the total analytical concentrations of components as primary variables (Kirkner and Reeves 1988):

$$\frac{\partial w_i}{\partial t} = \varphi(w_i) - \varphi(s_i) - \varphi(p_i) + r_i^w \;\; i = 1...N_c \qquad (2)$$

where w_i is the total analytical concentration of the ith mobile component ($M_m\ L^{-3}$), s_i is the total adsorbed concentration of the ith mobile component to biological solids ($M_m\ L^{-3}$), p_i is the total precipitated concentration of the ith mobile component ($M_m\ L^{-3}$), r_i^w is the rate of accumulation of the ith mobile component due to kinetic-controlled biological reactions ($M_m\ L^{-3}\ T^{-1}$), N_c is the number of components, and $\varphi()$ is the advection-dispersion operator. For 1-D saturated ground-water flow, $\varphi()$ is given by:

$$\varphi() = D\frac{\partial^2}{\partial x^2} - v\frac{\partial}{\partial x} \qquad (3)$$

where v is the ground-water velocity (LT^{-1}), D is the effective diffusion coefficient ($L^2\ T^{-1}$), and x is distance (L). We assume that adsorption and precipitation reactions are at thermodynamic equilibrium, while kinetics control biological reactions.

It is necessary to include mass balances on kinetic reactions involving immobile biological components, such as bacteria attached to the solid matrix:

$$\frac{\partial m_k}{\partial t} = r_k^m \quad k = 1...N_m \qquad (4)$$

where m_k is the concentration of the kth immobile biological component (M_i), r_k^m is the rate of accumulation of the kth immobile component due to biological processes ($M_iL^{-3}\ T^{-1}$), and N_m is the number of immobile biological components.

Solution of the reactive-transport problem requires discretizing the domain according to the integrated finite-difference formulation (Steefel and Lasaga 1994), assuming a constant-concentration boundary for the up-gradient end and a zero-concentration gradient boundary for the down-gradient end. We subdivide the domain in 60 control volumes.

The solution procedure is iterative. We use a Pickard-iteration scheme (Tebes-Stevens et al. 1998), to alternate between solution to reactive transport equations (Eqs. 2 and 4) and solution to the chemical-equilibrium problem. The key output of reactive transport equations is the spatial distribution of total analytical concentrations of mobile and immobile components. Surface-site densities are used then to update the concentration of functional groups required in chemical equilibrium calculations. Using the total analytical concentrations as input, the chemical equilibrium is solved for aqueous and surface complexation and for precipitation/dissolution reactions. The output of the chemical equilibrium problem is the spatial distribution of concentrations of all species (i.e., free components, aqueous complexes, surface complexes, and precipitates), which are then used to update the precipitated and adsorbed fractions of components and the rate of accumulation due to biological reactions, required in transport equations. The iteration procedure is halted when concentration changes between subsequent iterations are below a certain threshold; then, time is allowed to advance.

In order to obtain steady-state solutions, the expanded CCBATCH determines the evolution with time of all species, subject to initial conditions. Systems eventually reach steady state when concentrations changes of all species between subsequent times become negligible. This general rule has two exceptions. First, inert biomass concentration never stabilizes; only the rate of formation of inerts becomes constant, since it is proportional to the concentrations of active biomass, which approaches a steady state. Second, a mineral can precipitate even after concentrations of all aqueous species have reached steady state, since the steady-state biomass continues to produce chemical species that can precipitate (e.g., sulfide). We assume that the steady-state production rates in these two cases are sustainable for the lifetime of the system, and, hence, relevant for studying bio-protection. This assumption could be invalid if excessive accumulation of inerts or minerals were to clog the porous

medium, preventing the delivery of sulfate. Excessive accumulation of biomass leading to severe constriction of pores often occurs in the vicinity of substrate injection wells; however, clogging of the pores is less likely to occur in PRBs because of low biomass accumulation. In fact, the PRB at the Nickel Rim site operated for over 5 years without showing signs of clogging (Blowes et al. 2000).

Finally, the reactivity of the POM in PRBs will decrease over time, as the most reactive material is consumed first (Benner et al. 2002). For this case, definition of a steady state is more difficult, as species concentrations continually adjust to the level of reactivity of the POM. A model of organic-C reactivity would be necessary to predict the long-term trends of PRBs. We do not consider depletion of the POM in our analysis.

The solution approach we use with CCBATCH involves initializing the aqueous species of the system with inflowing concentrations, except for the inflowing metal concentration. We assume the metal to be absent in the system initially. We use the steady-state biomass estimates (Eq. 1) as initial biomass concentrations, which allows rapid establishment of the true steady-state biomasses and a reactive-ligand gradient capable of detoxifying the inflowing metal. This steady state occurs after about 50 days. We add metal to the up-gradient input from the start of the simulation. The time it takes the metal to reach the up-gradient boundary of the PRB is enough for the PRB to develop a sulfide counter gradient capable of detoxifying the inflowing metal.

Modeling results

We present results at steady state for two scenarios, with precipitation turned on or off. Precipitation turned on represents the expected situation for sulfidic systems, because sulfide mineral formation usually is fast. Alternatively, precipitation turned off might represent a sulfidic system with very slow precipitation kinetics. The primary reason we turn off precipitation is to define the relative importance of precipitation versus other bio-protection mechanisms.

The influent concentration of 50 μM Zn satisfies the analytical stability criterion for advection-dominated systems with precipitation (Schwarz and Rittmann 2006):

$$q_{\mathrm{A}} = \frac{rD_L}{u_{\mathrm{M0}}v^2} \geq 1 \tag{5}$$

where u_{M0} is the up-gradient constant total soluble-metal concentration (50 μM), D_L is the ligand's effective diffusion coefficient in the barrier (10^{-4} m^2 d^{-1}), v is the ground-water velocity (5 m y^{-1}), and r is the rate of ligand production (10^{-4} mol l^{-1} d^{-1}), which is equal to the rate of sulfate reduction introduced earlier. The corresponding q_A value (Eq. 5) for 50 μM influent Zn is 1.07. Thus, the 50-μM condition represents a limiting situation, because it just complies with the criterion ($q_A > 1$) for stable bio-protection. To gain a stable solution for no precipitation, we have to turn off Zn toxicity.

The first set of figures, which are identical for the two simulation scenarios, show biomass and SMP results. Figure 2 indicates that fermenting bacteria predominate due to their high yield. Inert biomass is not shown in Fig. 2, because they accumulate continually. While inerts are generated at low rates, they have no sink; thus, inerts might eventually become the dominant biomass type. The active biomass and EPS profiles are nearly constant within the PRB, because substrate becomes available at a uniform rate across the domain. The slight biomass increase toward the down-gradient end of the domain are due to

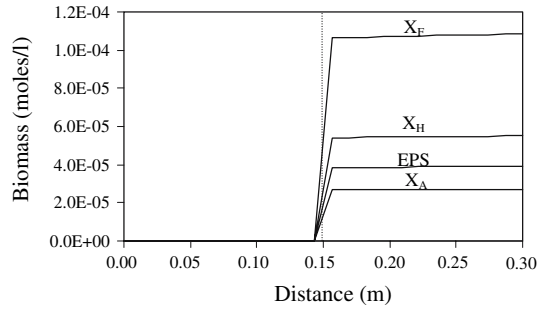

Fig. 2 Steady-state concentration profiles of active biomass components and EPS for an organic PRB subject to the hydrolysis rate k_{hl} of 4.75×10^{-5} mol cellulose l^{-1} d^{-1}. The dotted line indicates the up-gradient PRB boundary

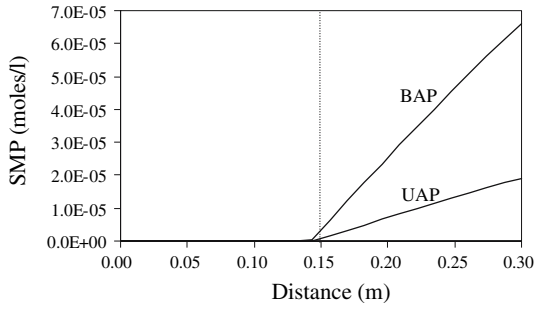

Fig. 3 SMP concentration profiles for an organic PRB subject to the hydrolysis rate k_{hl} of 4.7495×10^{-5} mol cellulose l^{-1} d^{-1}

production and consumption of SMP and their increasing concentration down-gradient. Figure 3 shows that SMP display a nearly linear concentration profile. The increasing trend is characteristic of solutes generated at uniform rates in advection-dominated environments. BAP dominate the soluble COD, which equals UAP + BAP.

pH changes can be significant in sulfidic systems, according to pH measurements of Benner et al. (1999) at the Nickel Rim PRB. There, a sulfidic consortium buffered the acidic ground water (up-gradient pH = 5.5) to a pH of 6.7. Our pH profiles (not shown) also converge to a pH of around 6.7, but speciation effects are not significant, because our influent pH (7.1) is close to the outflow pH.

Figures 4 and 5 show, respectively, the speciation results for Zn and sulfide for the case when precipitation is turned off. In the region

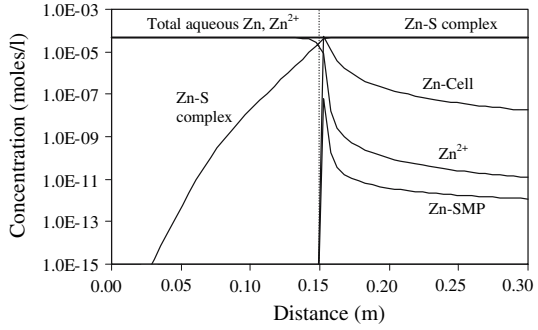

Fig. 4 Speciation of Zn for an influent Zn concentration of 50 μM, precipitation turned off, and Zn toxicity turned off. Zn-Cell denotes all immobile Zn associated with either inerts, EPS, or active cells

up-gradient of the PRB, most Zn is in the aqueous free form, while Zn-sulfide complexes dominate within the PRB (Fig. 4). In the presence of free sulfide, an extremely strong ligand, Zn^{2+} only barely associates with active cells, inerts, EPS (Zn-cell), and soluble microbial products (Zn-SMP).

Sulfide speciation is controlled by Zn-S complexation in the immediate vicinity of the up-gradient boundary of the PRB (Fig. 5). Farther up-gradient and down-gradient, most sulfide is in the free form. Figure 6, which combines the Zn and sulfide profiles, shows that total aqueous Zn and sulfide profiles intersect near the up-gradient boundary of the PRB, reducing the concentration of free metal. The metal, however, is not detoxified, and the PRB should fail if Zn toxicity were made active. In the up-gradient region of the barrier, Zn^{2+} concentrations are above typical toxicity thresholds for SRB, and, thus, the negative feedback mechanism between toxicity and ligand generation should cause the barrier to fail. In this simulation, we obtain the steady-state concentration profiles by switching off the toxicity function. However, switching on Zn toxicity leads to failure of the PRB as the Zn front gradually moves through the PRB (not shown).

Figures 7 and 8 show the speciation results for the more realistic case of a sulfidic system in which precipitation is turned on and rapid enough to go to equilibrium. Zn toxicity also is turned on. Figure 7, displaying the speciation of Zn, shows two distinctive features compared to the no-precipitation case (Fig. 4). In the vicinity of the up-gradient boundary of the PRB, most Zn is present as the sulfide mineral $ZnS_{(s)}$. Also, because a significant fraction of aqueous Zn is precipitating out of solution in this region, total aqueous Zn is reduced. The peak of the total Zn profile is not at steady state, as it increases with time due to mineral formation. This total Zn profile shown in Fig. 7 corresponds to conditions after 120 days of operating the PRB. On the other hand, similar to the no-precipitation case, Zn-sulfide complexes dominate Zn speciation within the PRB (Fig. 7).

As occurs for Zn, sulfide speciation in the vicinity of the up-gradient boundary of the PRB is

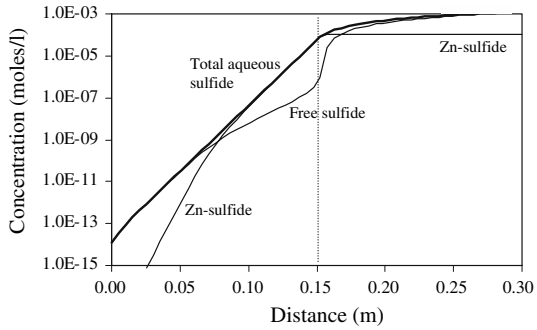

Fig. 5 Speciation of sulfide for a high inflowing Zn concentration and precipitation turned off. Free sulfide denotes the sum of H_2S, HS^-, and S^{2-}

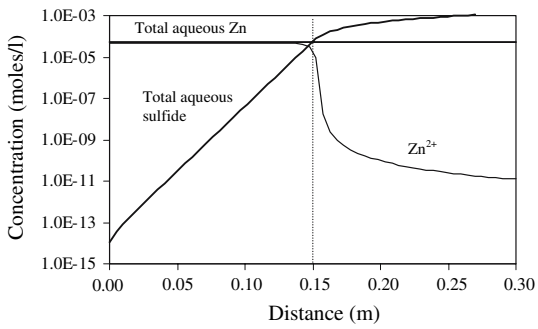

Fig. 6 Free Zn and total aqueous concentration profiles of Zn and sulfide for an influent Zn concentration of 50 μM and precipitation and Zn toxicity turned off

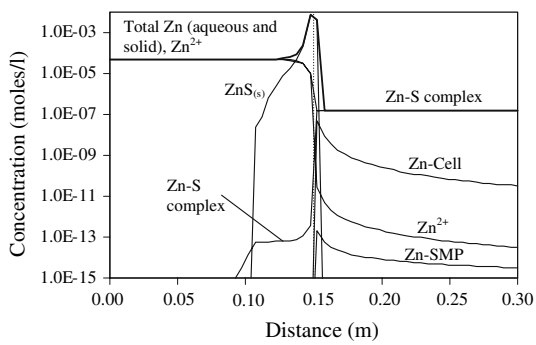

Fig. 7 Speciation of Zn for an influent Zn concentration of 50 μM and precipitation and Zn toxicity turned on. Zn-Cell denotes all immobile Zn associated with either inerts, EPS, and active cells. The total-Zn profile is for 120 days

controlled by the mineral phase (Fig. 8). Also, farther up-gradient and down-gradient, most sulfide is in the free form.

Figure 9 describes how the metal gradient and the sulfide counter gradient meet at the

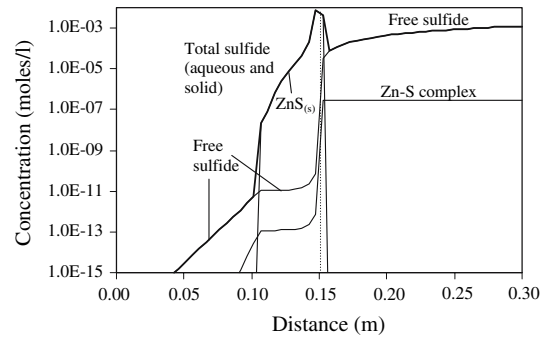

Fig. 8 Speciation of sulfide for an influent Zn concentration of 50 μM and precipitation turned on. Free sulfide denotes the sum of H_2S, HS^-, and S^{2-}. Simulation time = 120 days

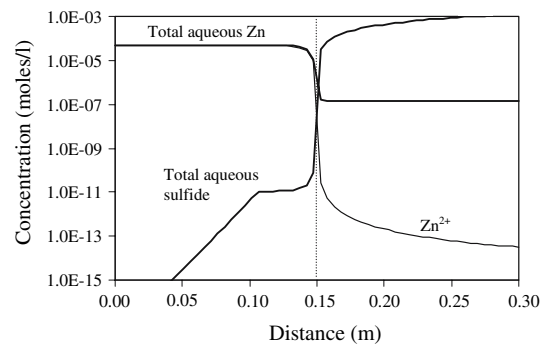

Fig. 9 Free Zn and total aqueous concentration profiles of Zn and sulfide for an influent Zn concentration of 50 μM and precipitation turned on

up-gradient boundary of the PRB. The metal is effectively detoxified, because free-metal concentrations in the up-gradient region of the barrier are below 10^{-7} M, a free-Zn concentration that is generally non-toxic to bacteria.

Conclusions

We use a comprehensive biogeochemical description of sulfidic systems with the computer program CCBATCH, allowing us for the first time unraveling their complex interactions with toxic metals when transport processes are significant. Specifically, we use the biogeochemical description of a sulfidic system with the CCBATCH program expanded to include transport processes, and we test the bio-protection hypothesis in much

more detail than we could using analytical modeling. Using a permeable reactive barrier as model system, we perform two kinds of numerical experiments, with and without precipitation of zinc-sulfide solids. Our modeling results show the importance of toxicant gradients as bio-protection mechanisms from metal toxicity in a 1-D groundwater environment. Comparing the results for the two precipitation scenarios shows the higher potential of precipitation in metal detoxification. Additionally, the detailed biogeochemical analysis confirms the relevance of sulfide as a detoxifying agent when transport is considered. High affinity for the metal, high rate of production, and high mobility are the three properties of sulfide that are key to a bio-protection mechanism based on chemical gradients. Finally, a metal-resistance criterion developed from an analytical solution is accurate for defining when bio-protection should work when applied to this more realistic scenario.

References

Benner SG, Blowes DW, Gould WD et al (1999) Geochemistry of a permeable reactive barrier for metals and acid mine drainage. Environ Sci Technol 33(16):2793–2799

Benner SG, Blowes DW, Ptacek CJ, Mayer KU (2002) Rates of sulfate reduction and metal sulfide precipitation in a permeable reactive barrier. Appl Geochem 17:301–320

Blowes DW, Ptacek CJ, Benner SG et al (2000) Treatment of inorganic contaminants using permeable reactive barriers. Contam Hydrol 45:123–137

Campbell PGC (1995) Interactions between trace metals and organisms: critique of the free-ion activity model. In: Tessier A, Turner D (eds) Metal speciation and bioavailability in aquatic systems. Wiley, Chichester, UK

Campbell PGC, Errecalde O, Fortin C, Hiriart-Baer VP, Vigneault B (2002) Metal bioavailability to phytoplankton – applicability of the biotic ligand model. Comp Biochem Physiol Part C 133:189–206

Kirkner DJ, Reeves H (1988) Multicomponent mass transport with homogeneous and heterogeneous chemical reactions: effect of the chemistry on the choice of numerical algorithm, 1. Theory. Water Resour Res 24(10):1719–1729

Paquin PR, Gorsuch JW, Apte S et al (2002) The biotic ligand model: a historical overview. Comp Biochem Physiol Part C 133:3–35

Rittmann BE, McCarty PL (2001) Environmental biotechnology: principles and applications. McGraw-Hill, New York

Schwarz AO, Rittmann BE (2007) A biogeochemical framework for metal detoxification in sulfidic systems. Biodegradation (in press). doi: 10.1007/s10532-007-9101-2

Schwarz AO, Rittmann BE (2006) Analytical-modeling analysis of how pore-water gradients of toxic metals confer community resistance. Adv Water Res (in press). doi: 10.1016/j.advwatres.2006.05.015

Steefel CI, Lasaga AC (1994) A coupled model for transport of multiple chemical species and kinetic precipitation/dissolution reactions with application to reactive flow in single phase hydrothermal systems. Am J Sci 294:529–592

Stumm W, Morgan JJ (1996) Aquatic chemistry. John Wiley & Sons, New York

Tebes-Stevens C, Valocchi AJ, Van Briesen JM, Rittmann BE (1998) Multicomponent transport with coupled geochemical and microbiological reactions: model description and example simulations. J Hydrol 209:8–26

Waybrant KR, Ptacek CJ, Blowes DW (2002) Treatment of mine drainage using permeable reactive barriers: column experiments. Environ Sci Technol 36:1349–1356